Photochemistry and Photobiology, 20**, **: *–*

Photoinduced Oxidation of Sterically Hindered Amines in Acetonitrile Solutions and Titania Suspensions (An EPR Study)

Zuzana Barbieriková, Mária Mihalíková and Vlasta Brezová*

Institute of Physical Chemistry and Chemical Physics, Faculty of Chemical and Food Technology, Slovak University of Technology, Bratislava, Slovakia

Received 12 March 2012, accepted 12 June 2012, DOI: 10.1111/j.1751-1097.2012.01189.x

ABSTRACT

The reactions of sterically hindered amines (SHA) were investigated in acetonitrile solutions and TiO_2 suspensions upon exposure to monochromatic radiation, $\lambda = 365$ nm, by means of *in situ* EPR spectroscopy. The formation of singlet oxygen, as one of the possible oxidation agents for SHA, in these systems is affected significantly by solvent used and the experimental conditions. Experiments in homogeneous media evidenced alternative pathways for the SHA oxidation with a variety reactive oxygen species involved. In anhydrous acetonitrile solutions containing KO_2, the SHA oxidation was negligible not only in the dark but also on continuous exposure. However, the presence of water, even at low concentrations, led to the transformation of $O_2^{\bullet-}$ to singlet oxygen and hydrogen peroxide, which served as a source of hydroxyl radicals. These species participated in oxidation of SHA resulting in the generation of nitroxide radicals. To investigate the influence of different competitive reactions of SHA with other ROS formed upon TiO_2 photoexcitation, a series of experiments using different additives (*e.g.* KO_2, H_2O_2, NaN_3, dimethylsulfoxide, methanol as organic cosolvents) under air or argon were performed. The detailed analysis of paramagnetic intermediates formed upon the irradiation of the studied systems was accomplished using EPR spin trapping technique.

Abbreviations: **ACN, acetonitrile; BHT, 2,6-di-*tert*-butyl-4-methylphenol; c_{rel}, relative concentration; DMPO, 5,5-dimethyl-1-pyrroline *N*-oxide; DMSO, dimethylsulfoxide; EPR, electron paramagnetic resonance; Hfcc, hyperfine coupling constants; NS, number of scans; ROS, reactive oxygen species; SHA, sterically hindered amines; SW, magnetic field sweep width; TMP, 4-hydroxy-2,2,6,6-tetramethylpiperidine; TMPO, 4-oxo-2,2,6,6-tetramethylpiperidine; Tempol, 4-hydroxy-2,2,6,6-tetramethylpiperidine *N*-oxyl; Tempone, 4-oxo-2,2,6,6-tetramethylpiperidine *N*-oxyl; UV/Vis, ultraviolet/visible.**

INTRODUCTION

Various types of reactive oxygen species (ROS) and their degradation products are reported to be generated in heterogeneous systems of TiO_2 photocatalysts upon photoexcitation (1–4). All these intermediates, such as superoxide radical anion, hydroxyl radical or singlet oxygen, represent significantly reactive species especially when present in biological systems (5–7). Hydroxyl radicals denote an important ROS in the photodegradation of organic pollutants and other substances that possess a weak affinity for the titania surface. OH radicals are produced through the oxidation of surface hydroxyl groups or adsorbed water molecules by the photogenerated valence band holes. Superoxide radical anions are readily generated from molecular oxygen by capturing an electron from the conduction band of photoactivated titania. Although this species is of less importance in the initiation of oxidation reactions it mainly participates in the total mineralization of organic compounds, *e.g. via* the production of hydrogen peroxide by $O_2^{\bullet-}$ disproportionation (1). The specific mechanism for the formation of $^1O_2$ is not that straightforward, and different sources of singlet oxygen in these systems have been suggested (8,9). Singlet oxygen is expected to be formed *via* several different mechanisms:

(1) Energy transfer (Eq. [1])

$$TiO_2 \xrightarrow{h\nu} TiO_2^* \xrightarrow{O_2} TiO_2 + {}^1O_2 \quad (1)$$

(2) $HO_2^{\bullet}$ radical recombination (Eqs. [2] and [3])

$$TiO_2 + O_2 \xrightarrow{h\nu} O_2^{\bullet-} \xrightarrow{H^+} HOO^{\bullet} \quad (2)$$

$$2HOO^{\bullet} \rightarrow H_2O_2 + {}^1O_2 \quad (3)$$

(3) Oxidation of $O_2^{\bullet-}$ by the photogenerated hole h^+ (Eq. [4])

$$TiO_2 + O_2 \xrightarrow{h\nu} O_2^{\bullet-} \xrightarrow{h^+} {}^1O_2 \quad (4)$$

As photocatalysis and the photocatalysts themselves are becoming widely used in different areas of everyday life (air and water purification, building cleaning materials, etc.; 2,10); understanding the specific mechanisms of the formation and further reactivity of these species becomes essential regarding their effect on the processes on titania surfaces together with their environmental impact (11).

Several studies dealing with the formation of ROS in TiO_2 suspensions have been conducted, each adopting a slightly different approach. When electron paramagnetic resonance (EPR) spectroscopy is applied to the study of such systems mainly indirect ways of observing the reactive intermediates are available, which, in the case of paramag-

*Corresponding author email: vlasta.brezova@stuba.sk (Vlasta Brezová)

netic species, represents the spin trapping technique. The trapping of short lived species with nitrone, *N*-oxide or nitroso spin trapping agents results in the formation of more stable radicals, spin adducts, the EPR spectrum of which can give information about the structure and character of added species (1,12). However, this method is significantly dependent upon the choice of spin trap and experimental conditions and consequently much attention must be taken during the deduction of the reaction mechanisms on the basis of the observed spectra. One method to determine singlet oxygen generation is the direct detection of the phosphorescence at 1270 nm. Considering the significant dependence of singlet oxygen formation and its lifetime on the experimental conditions (*e.g.* solvent) various indirect methods have been developed, which however pose significant drawbacks when applied to the heterogeneous systems of photocatalysts (13).

Konaka *et al.* have examined the formation of singlet oxygen and the superoxide radical anion in irradiated ethanol TiO_2 suspensions by means of EPR spectroscopy (14). The generation of $^1O_2$ was confirmed by the oxidation of 4-oxo-2,2,6,6-tetramethylpiperidine (TMPO) to the paramagnetic species 4-oxo-2,2,6,6-tetramethylpiperidine *N*-oxyl (Tempone) and, to monitor the presence of $O_2^{\bullet-}$, the spin trapping agent DMPO was used. The authors observed the effect of the DMPO spin trap addition on the singlet oxygen formation. The fact that the concentration of Tempone increases with the increasing concentration of the spin trap in the systems shows that singlet oxygen is most probably formed on the surface of irradiated titania and its formation *via* the superoxide radical anion was excluded. Nosaka *et al.* (15) have conducted studies on the formation of singlet oxygen in aqueous TiO_2 suspensions by monitoring the intensity of its characteristic phosphorescence at 1270 nm. Detailed studies on the effect of KBr, KSCN, KI, H_2O_2 and ethanol on the concentration of singlet oxygen and the superoxide radical anion, monitored by chemiluminescence measurements with luminol, confirmed that singlet oxygen was generated *via* the reaction of a photogenerated hole with the superoxide radical anion, arising from the reduction of molecular oxygen by a photogenerated electron. The widely applied method for the determination of singlet oxygen by the oxidation of sterically hindered amines (SHA) seems not to be specific in systems where a variety of ROS are formed, hence they can take part in the reactions with SHA (16–18).

Previously, we have intensively investigated novel synthesized heterocyclic molecules (quinolones and selenadiazoloquinolones) possessing ability to activate molecular oxygen upon UVA photoexcitation, unfortunately characterized with limited solubility in water. During these investigations we revealed that anhydrous acetonitrile (ACN) represents a suitable solvent for the detection of singlet oxygen generation *via* monitoring SHA oxidation to nitroxide by EPR spectroscopy (19,20). Now, by applying *in situ* EPR spectroscopy we have investigated the reactions of SHA in acetonitrile solutions and TiO_2 suspensions upon exposure to monochromatic, $\lambda = 365$ nm, radiation. In accordance with previous studies and the literature we take into account that the oxidation of SHA to nitroxide radicals may take place *via* different pathways with different reactive species involved. In addition, the generation of $^1O_2$ under the given experimental conditions is significantly influenced by the solvent properties, as well as by competitive reactions of the ROS produced in the system. The identification of paramagnetic intermediates formed during the photoexcitation was performed using the EPR spin trapping technique. The addition of different reagents and solvents into the reaction system, together with the variation of experimental conditions provided information about potential SHA oxidation mechanisms in acetonitrile.

MATERIALS AND METHODS

Chemicals and reagents. The commercial titanium dioxide Aeroxide® P25 (Evonik Degussa, Germany) was used. All solutions and suspensions were prepared in dried ACN (SeccoSolv®; Merck). The stock TiO_2 suspensions containing 2 mg TiO_2 L^{-1} were homogenized for 2 min using ultrasound (Ultrasonic Compact Cleaner TESON 1; Tesla Piešťany, Slovakia). The spin trapping agent 5,5-dimethyl-1-pyrroline *N*-oxide (DMPO; Aldrich) was distilled before application and stored at −18°C. Hindered amines, *i.e.* 4-hydroxy-2,2,6,6-tetramethylpiperidine (TMP) and TMPO from Merck–Schuchardt were used as supplied. The concentration of photogenerated paramagnetic species was determined using solutions of 4-hydroxy-2,2,6,6-tetramethylpiperidine *N*-oxyl (Tempol; Aldrich) or Tempone (Aldrich) as calibration standards. Eosin Y (disodium salt; Sigma–Aldrich) was used as photosensitizer; sodium azide (analytical grade; Sigma–Aldrich) and 2,6-di-*tert*-butyl-4-methylphenol (BHT; Aldrich) were used as singlet oxygen quenchers. Dimethylsulfoxide (DMSO, SeccoSolv®; Merck), methanol (spectroscopic grade; Lachema, Czech Republic) or distilled water was added to ACN as a cosolvent. Potassium superoxide (Sigma–Aldrich), $AgNO_3$ (analytical grade; Lachema) and hydrogen peroxide (medical extra pure, *ca* 35%; Merck) were used without purification. The accurate concentration of H_2O_2 was determined spectrophotometrically by measuring the absorbance at 240 nm ($\varepsilon_{240} = 43.6$ м$^{-1}$ cm^{-1}; 21) by means of a Shimadzu UV-3600 UV/Vis/NIR spectrometer (Japan).

EPR in situ photochemical experiments. The formation of paramagnetic intermediates upon monochromatic irradiation ($\lambda = 365$ nm) of suspensions or solutions was monitored *in situ* using an EPR spectrometer, EMX Plus (Bruker, Germany). The samples containing hindered amines and/or DMPO were mixed directly before the EPR measurements, then carefully saturated with air, argon or oxygen using a slight gas stream and immediately transferred to a small quartz flat cell (WG 808-Q, optical cell length 0.04 cm; Wilmad-LabGlass) optimized for the TE_{102} cavity (Bruker, Germany). The samples were irradiated at 295 K directly in the EPR resonator, and the EPR spectra recorded *in situ* during continuous photoexcitation. All the EPR experiments were carried out at least in triplicate; with standard deviation in the relative EPR intensity of ±10%. The irradiation source was an UV LED monochromatic radiator ($\lambda = 365$ nm; Hönle UV Technology). The value of the irradiance (18 mW cm^{-2}; $\lambda = 365$ nm) within the EPR cavity was determined using a UVX radiometer (UVP, USA). In some cases, argon saturation needed to be applied after the irradiation of the aerated solutions/suspensions prior to the subsequent EPR experiment to get better resolved spectra by suppressing the line-broadening effect of molecular oxygen. The concentration of photogenerated paramagnetic species was evaluated from the double-integrated EPR spectra based on the calibration curve obtained from the EPR spectra of Tempol or Tempone solutions measured under strictly identical experimental conditions.

Typical EPR spectrometer settings in a standard photochemical experiment were: microwave frequency, *ca* 9.424 GHz; microwave power, 10.53 mW; center field, 335.6 mT; sweep width, 6–10 mT; gain, 2×10^5 to 1×10^6; modulation amplitude, 0.025–0.1 mT; scan, 17 s; time constant, 5.12–81.92 ms. The *g*-values were determined using a built-in magnetometer. The EPR spectra so obtained were analyzed and simulated using the Bruker software WinEPR and SimFonia and the Winsim2002 software freely available from the website of the National Institute of Environmental Health Sciences (NIEHS; http://epr.niehs.nih.gov/; 22).

RESULTS AND DISCUSSION

Oxidation of TMP and TMPO by the superoxide radical anion, hydrogen peroxide and the hydroxyl radical

Oxidation of SHA with EPR detection of photogenerated nitroxide radicals (in combination with singlet oxygen quenchers and with application of deuterated solvents) represents a frequently used technique for the detection of $^1O_2$ upon the photoexcitation of various photoactive compounds (16,19,20,23). For illustration we performed, under the given experimental conditions (λ = 365 nm), *in situ* photoexcitation of the well-known photosensitizer Eosin Y (24) in aerated solutions containing TMP, as well as after addition of the singlet oxygen quencher sodium azide (Fig. 1). Due to the limited solubility of NaN_3 in acetonitrile, the experiments were performed in acetonitrile containing 4% (by vol) of water. Photoexcitation causes the generation of a three-line EPR signal characteristic of the nitroxide radical (a_N = 1.73 mT; g = 2.0060), that is fully suppressed upon addition of NaN_3 (Fig. 1). It should be noted here that the high solubility of molecular oxygen in acetonitrile (25) caused broadening of spectral lines (peak-to-peak linewidth, ΔB_{pp} = 0.25 mT).

However, as was mentioned elsewhere, the selectivity of sterically hindered amine oxidation by singlet oxygen resulting in the generation of paramagnetic nitroxide radicals still remains open to question (17,26–28). As the UVA photoexcitation of TiO_2 particles leads to the formation of different ROS, *e.g.* $O_2^{\bullet-}$/$^\bullet$OOH, H_2O_2, $^\bullet$OH, in addition to $^1O_2$ (1,29), we performed a set of EPR experiments with KO_2 and H_2O_2 in the dark and subsequently upon monochromatic photoexcitation (λ = 365 nm) to investigate their role in the oxidation of TMP and TMPO.

The solutions of KO_2 in aprotic solvents (DMSO, ACN) represent a well-defined source of superoxide radical anions (30), as we also confirmed in acetonitrile solutions *via* spin trapping experiments using DMPO (Fig. 2a). The EPR spectra obtained in deaerated KO_2 solutions (freshly prepared using dried ACN) in the presence of DMPO are fully compatible with the presence of the $^\bullet$DMPO-O_2^- spin adduct, which is characterized with spin Hamiltonian parameters a_N = 1.289 mT, a_H^β = 1.038 mT, a_H^γ = 0.130 mT; g = 2.0059 (31). However, in addition low-intensity spectra attributed to oxygen-centered ($^\bullet$DMPO-OR; a_N = 1.370 mT, a_H^β = 1.197 mT, a_H^γ = 0.088 mT; g = 2.0059) and carbon-centered spin adducts ($^\bullet$DMPO-CR; a_N = 1.407 mT, a_H^β = 2.111 mT; g = 2.0057) were found in the experimental spectra (Fig. 2a). These spin adducts probably resulted from the interaction of DMPO with an intermediate produced in the reaction of acetonitrile

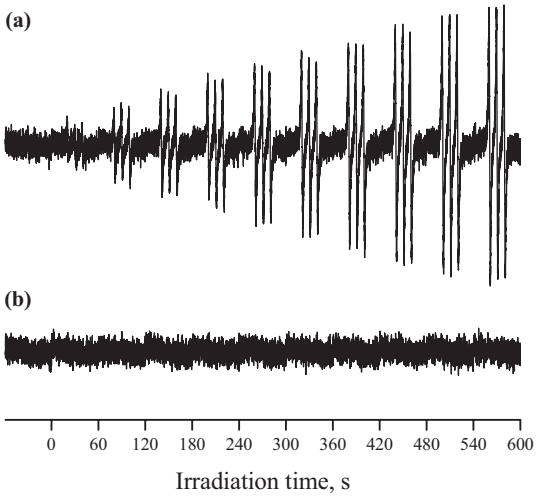

Figure 1. (a) Time evolution of the electron paramagnetic resonance (EPR) spectra (SW = 10 mT) observed upon monochromatic irradiation (λ = 365 nm) of photosensitizer Eosin Y (c_0[Eosin Y] = 0.76 mM) in aerated ACN/water solution (water 4%; vol) in the presence of 0.01 M 4-hydroxy-2,2,6,6-tetramethylpiperidine (TMP). (b) Influence of sodium azide in an experiment analogous to (a) with the addition of NaN_3 ($c_0(NaN_3)$ = 4 mM).

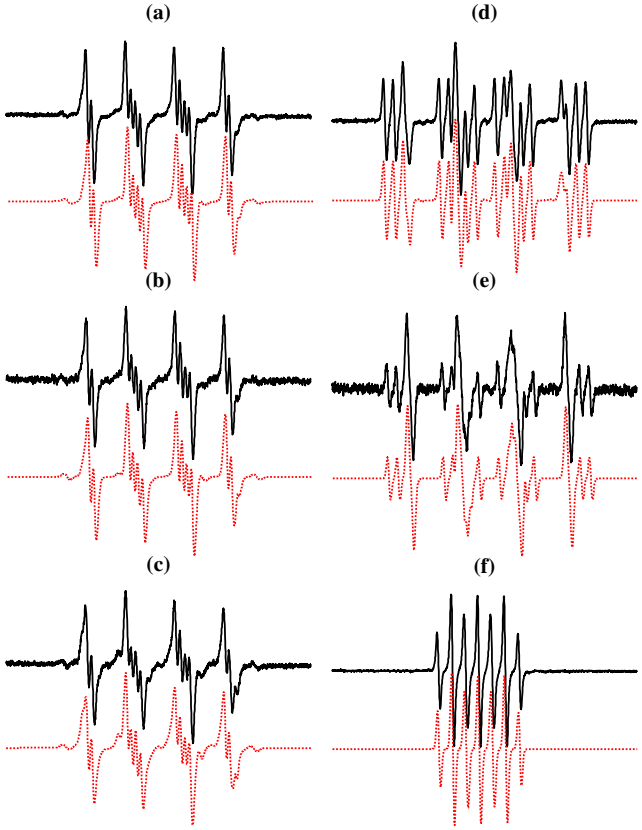

Figure 2. Experimental (solid line) and simulated (dotted line) EPR spectra (SW = 8 mT) obtained in the deoxygenated acetonitrile solutions of KO_2 in the presence of the DMPO spin trap: (a) dark; upon the irradiation of (b) 60 s, (c) 600 s, (d) in the mixed solvent ACN/water (water 40%; vol) in the dark and upon the irradiation of (e) 60 s, (f) 600 s. Initial concentrations: $c_0(KO_2)$ = 0.001 M, c_0(DMPO) = 0.04 M; irradiation wavelength 365 nm. Simulation parameters: (a) $^\bullet$DMPO-O_2^- (a_N = 1.289 mT, a_H^β = 1.038 mT, a_H^γ = 0.130 mT; g = 2.0059; rel. conc. 79%), $^\bullet$DMPO-OR (a_N = 1.370 mT, a_H^β = 1.197 mT, a_H^γ = 0.088 mT; g = 2.0059; 13%), $^\bullet$DMPO-CR (a_N = 1.407 mT, a_H^β = 2.111 mT; g = 2.0057; 8%); (b) $^\bullet$DMPO-O_2^- (80%), $^\bullet$DMPO-OR (16%), $^\bullet$DMPO-CR (4%); (c) $^\bullet$DMPO-O_2^- (87%), $^\bullet$DMPO-OR (8%), $^\bullet$DMPO-CR (3%), $^\bullet$DMPO-$_{degr}$ (a_N = 1.397 mT; g = 2.0059; 2%); (d) $^\bullet$DMPO-O_2^-/OOH (a_N = 1.418 mT, a_H^β = 1.298 mT, a_H^γ = 0.068 mT; g = 2.0059; 41%), $^\bullet$DMPO-NR ($a_{N(NO)}$ = 1.464 mT, a_H^β = 1.895 mT, a_N = 0.251 mT; g = 2.0058; 58%), $^\bullet$DMPO$_{degr}$ (a_N = 1.748 mT; g = 2.0058; 1%); (e) $^\bullet$DMPO-O_2^-/OOH (63%), $^\bullet$DMPO-NR (28%), $^\bullet$DMPO-OH (a_N = 1.406 mT, a_H^β = 1.312 mT, a_H^γ = 0.098 mT; g = 2.0059; 9%); (f) $^\bullet$DMPO-X (a_N = 0.694 mT, a_H^γ(2H) = 0.369 mT; g = 2.0069; 100%).

with superoxide radical anions (32) or with the $O_2^{\bullet-}$ decomposition products (33). Irradiation (λ = 365 nm) of deaerated KO_2/ACN/DMPO solutions caused changes in the relative concentrations of the spin adducts, and upon longer exposure also the generation of an additional three-line EPR signal of negligible intensity ($^{\bullet}DMPO_{degr}$; a_N = 1.397 mT; g = 2.0059) originating from the DMPO degradation (Fig. 2b,c).

Sterically hindered amines TMP or TMPO were added to the KO_2 solutions freshly prepared using dried ACN, and the generation of the paramagnetic signals of nitroxide under either argon or air was monitored *in situ*, firstly in the dark (720 s) and subsequently on continuous irradiation (600 s), as shown in Fig. 3 (open squares). Under the given experimental conditions, the concentration of generated nitroxide Tempol and Tempone was negligible (< 1 μM). Therefore, in accordance with the literature (26) we can conclude that in the water-free ACN solutions superoxide radical anions do not oxidize SHA to nitroxides. However, a small amount of water in the acetonitrile KO_2 solution can significantly change the reaction mechanism. The presence of 4% (by vol) of water in acetonitrile induces oxidation of TMP or TMPO in dark, and a substantial increase of nitroxide concentration was observed upon the exposure to 365 nm radiation (Fig. 3). Further increase of water content in ACN resulted in a notable increase of nitroxide concentration especially upon irradiation (Fig. 3). However, with the highest water ratio (40%; vol), a limitation in the increase in $>NO^{\bullet}$ concentration was observed during irradiation, which can be caused by: (1) decomposition of the superoxide radical anion in aqueous media (34,35), (2) differences in the lifetime of singlet oxygen in water (4.6 μs) and in acetonitrile (71 μs; 36) and (3) the consecutive reactions of photogenerated nitroxides with ROS producing diamagnetic compounds (12,37–39).

Previously, Corey *et al.* (34) reported the characteristic emission of singlet oxygen at 1268 nm from KO_2 after addition of water to aprotic halogenated solvents, and the following reaction mechanism was proposed (Eqs. [5] and [6]):

$$O_2^{\bullet-} + H_2O \longrightarrow HO^- + HOO^{\bullet} \xrightarrow{O_2^{\bullet-}} HOOOO^- \longrightarrow HOO^- + {}^1O_2 \quad (5)$$

$$2\ HOO^{\bullet} + H_2O \longrightarrow HOOH + H_2O + {}^1O_2 \quad (6)$$

However, the generation of singlet oxygen *via* the interaction with peroxyl radicals produced in the reactions of the halogenated solvents with KO_2 may represent an alternative mechanism as was mentioned in (40).

The oxidation of TMP producing nitroxide radicals shown in Fig. 3 suggests that the presence of water in acetonitrile, even at low concentrations, significantly influenced the reactivity of KO_2. We propose that in solutions of KO_2/ACN/-water in the dark the generation of nitroxide radicals from TMP or TMPO is caused by singlet oxygen or hydrogen peroxide (34,41) produced in accordance with Eqs. [5] and [6]. However, we should keep in mind that SHA are widely used as polymer stabilizers, with the main stabilization effect previously attributed to the ability of nitroxide radicals, generated *via* their oxidation, to recombine the active radicals produced upon degradation (42,43). Theoretically, also here we can consider further alternative mechanisms of TMP or TMPO oxidation, *e.g.* interactions of SHA with peroxyl and alkoxyl radicals from solvent. The generation of spin adducts $^{\bullet}$DMPO-OR, $^{\bullet}$DMPO-CR was observed in dark and upon 365 nm exposure in system KO_2/DMPO/ACN (Fig. 2a–c), where only negligible oxidation of SHA to nitroxide was found. These results are in accord with the previous investigations, in which to this reaction pathway of SHA oxidation less importance was attributed (44–46).

Singlet oxygen can be produced *via* interaction of the superoxide radical anion and hydrogen peroxide (47). Upon photoexcitation of KO_2/ACN/water with 365 nm radiation, photolysis of hydrogen peroxide results in the generation of hydroxyl radicals, that may also initiate oxidation of SHA to nitroxides (17).

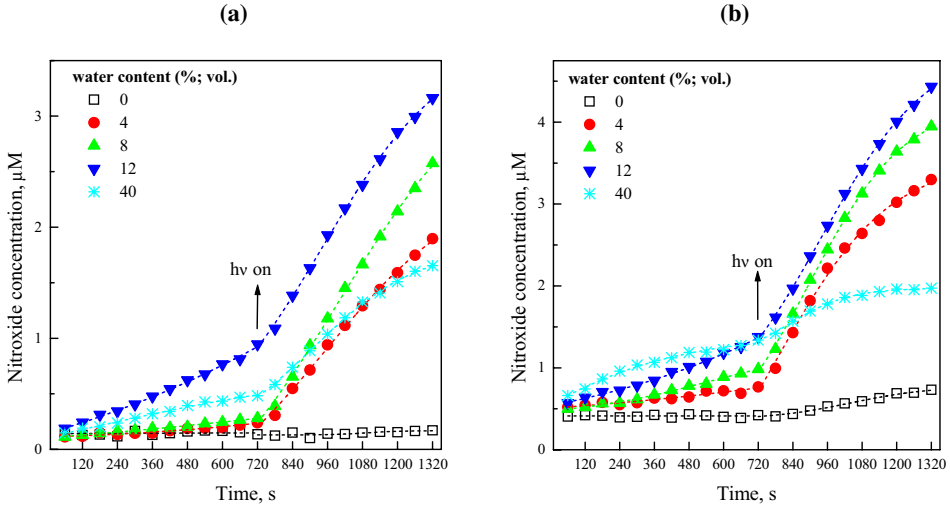

Figure 3. Time dependence of the concentration of nitroxide produced *via* TMP oxidation in KO_2 acetonitrile/water solutions monitored in the dark and on continuous irradiation: (a) under air; (b) under argon. Initial concentrations: $c_0(KO_2)$ = 0.001 M, c_0(TMP) = 0.01 M; irradiation wavelength 365 nm. The symbols represent the experimental data and the dashed lines their mathematical simulations using least squares analysis.

The detailed analysis of the experimental EPR spectra measured in the solution KO_2/TMP/ACN/water/argon upon irradiation confirmed the generation of two nitroxide radicals, *i.e.* Tempol (a_N = 1.653 mT; g = 2.0060) and Tempone (a_N = 1.546 mT; g = 2.0060), as is depicted in Fig. 4a. Analogous experiments performed in the irradiated solutions KO_2/TMPO/ACN/water/argon evidenced exclusively generation of Tempone (Fig. 4b). Previously, it was shown that Tempol can be oxidized to Tempone by hydroxyl radicals (48); the recent investigations pointed to the dominant role of singlet oxygen in the oxidation of TMP to Tempol and Tempone (49). As the formation of both reactive agents ($^1O_2$ and $^\bullet$OH) is probable under the experimental conditions used in our study, the exact determination of oxidation mechanism is not possible. It should be noted here that in the solutions KO_2/TMP/ACN/water/air significant line broadening of the EPR spectra excludes the confirmation of the simultaneous formation of Tempol and Tempone.

The behavior of KO_2 in acetonitrile/water (40% by vol) was analyzed by a spin trapping technique using DMPO (Fig. 2d–f). In the solution KO_2/DMPO/ACN/water/argon in the dark we observed EPR signals attributed to $^\bullet$DMPO-O_2^-/OOH (a_N = 1.418 mT, a_H^β = 1.298 mT, a_H^γ = 0.068 mT; g = 2.0059), $^\bullet$DMPO-NR ($a_{N(NO)}$ = 1.464 mT, a_H^β = 1.895 mT, a_N = 0.251 mT; g = 2.0058), together with a three-line signal of low intensity assigned to a degradation product of DMPO (Fig. 2d). Under aprotic conditions, $O_2^{\bullet-}$ behaves as a strong nucleophile and can react with acetonitrile (32,35). Superoxide radical anions remove protons from water and disproportionate producing singlet oxygen and hydrogen peroxide (Eqs. [5] and [6]; 35). We propose that the $^\bullet$DMPO-NR spin adduct, evidenced in the experimental EPR spectra, is generated *via* the trapping of free radicals produced in the reaction of $O_2^{\bullet-}$ or its degradation products with acetonitrile (33). The EPR spectra measured upon irradiation of solutions KO_2/DMPO/ACN/-water/argon were dependent on the water content, as well as on the irradiation time. EPR spectrum in Fig. 2e was measured after 60 s exposure and its simulation corresponds to a linear combination of three spin adducts, *i.e.* $^\bullet$DMPO-O_2^-/OOH (63%), $^\bullet$DMPO-NR (28%), $^\bullet$DMPO-OH (a_N = 1.406 mT, a_H^β = 1.312 mT, a_H^γ = 0.098 mT; g = 2.0059; 9%). After 600 s of irradiation these EPR signals disappeared and typical seven-line EPR spectrum of $^\bullet$DMPO-X spin adduct (a_N = 0.694 mT, a_H^γ(2H) = 0.369 mT; g = 2.0069) was observed (Fig. 2f). It should be noted here, that the hyperfine coupling constants of $^\bullet$DMPO-OH spin adduct in the presence of aprotic solvents significantly differ (50) from the typical four-line EPR signal (a_N = 1.490 mT, a_H^β = 1.490 mT; g = 2.0059) monitored in water (12,51). The oxidation of spin trapping agent DMPO to $^\bullet$DMPO-X was previously described in the systems possessing high-oxidation facility (6,12,52,53). Also here, irradiation of KO_2/DMPO/ACN/water under argon led to the generation of ROS capable to oxidize spin trapping agent *via* paramagnetic intermediate to $^\bullet$DMPO-X (Fig. 2f).

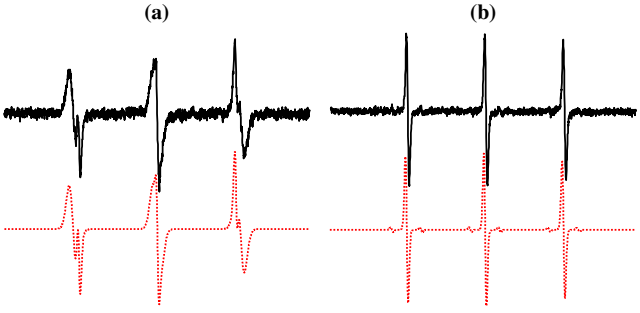

Figure 4. Experimental (solid line) and simulated (dotted line) EPR spectra (SW = 6 mT) obtained after 600 s exposure in the deoxygenated mixed solvent ACN/water (water 40%; vol) in the presence of KO_2 and: (a) TMP, (b) TMPO. Initial concentrations: $c_0(KO_2)$ = 0.001 M, c_0(TMP) = 0.01 M, c_0(TMPO) = 0.01 M; irradiation wavelength 365 nm. Simulation parameters: (a) Tempol (a_N = 1.653 mT; g = 2.0060; 89%), Tempone (a_N = 1.546 mT; g = 2.0060; 11%); (b) Tempone (a_N = 1.550 mT; $a_{13C}(4^{13}C)$ = 0.575 mT; g = 2.0060; 100%).

As hydrogen peroxide represents a product of KO_2 interaction in ACN/water solutions (Eqs. [5] and [6]), the role of H_2O_2 in the oxidation of SHA in acetonitrile was monitored in the dark (720 s) and on continuous exposure (600 s, λ = 365 nm) as is shown in Fig. 5. In solutions of H_2O_2/TMP/ACN under air or argon nearly analogous behavior was observed. Under dark conditions, the Radziszewski reaction of H_2O_2 with acetonitrile in the presence of TMP may generate singlet oxygen (41). However, the hydrogen peroxide concentration range (0.023–0.180 M) applied in our study caused only negligible increase in the concentration of nitroxide radicals during 720 s (Fig. 5). The start of irradiation (λ = 365 nm) caused immediate generation of a three-line EPR signal attributable to nitroxides, and the concentration increase observed during a 600 s exposure was proportional to the initial H_2O_2 concentrations (Fig. 5).

Photolysis of hydrogen peroxide initiates the production of hydroxyl radicals, as well as further ROS (Eqs. [7]–[11]), capable of oxidizing TMP and TMPO producing nitroxide radicals.

$$H_2O_2 \xrightarrow{h\nu} 2^\bullet OH \quad (7)$$

$$^\bullet OH + H_2O_2 \longrightarrow H_2O + ^\bullet OOH \quad (8)$$

$$^\bullet OOH \leftrightarrow O_2^{\bullet-} + H^+ \quad (9)$$

$$^\bullet OOH + H_2O_2 \longrightarrow H_2O + ^\bullet OH + O_2 \quad (10)$$

$$2^\bullet OOH \longrightarrow H_2O_2 + {}^1O_2 \quad (11)$$

Molecular oxygen may be produced in the processes of singlet oxygen quenching (36) also in argon saturated solutions, *e.g.* the superoxide radical anion is a very effective quencher of singlet oxygen (54).

To understand the role of hydroxyl radicals in the oxidation of SHA, we performed further experiments in a mixed solvent acetonitrile/DMSO (20%; vol). Acetonitrile reacts with hydroxyl radicals significantly slower (55) than DMSO (56; Eqs. [12] and [13]; 57). According to the literature, acetonitrile has the lowest rate constant for reacting with hydroxyl radicals among commonly used organic solvents (58).

$$CH_3CN + ^\bullet OH \xrightarrow{k=2.2\times10^7 M^{-1}S^{-1}} \text{products} \quad (12)$$

$$(CH_3)_2SO + ^\bullet OH \xrightarrow{k=7.0\times10^9 M^{-1}S^{-1}} CH_3(OH)SO + \bullet CH3 \quad (13)$$

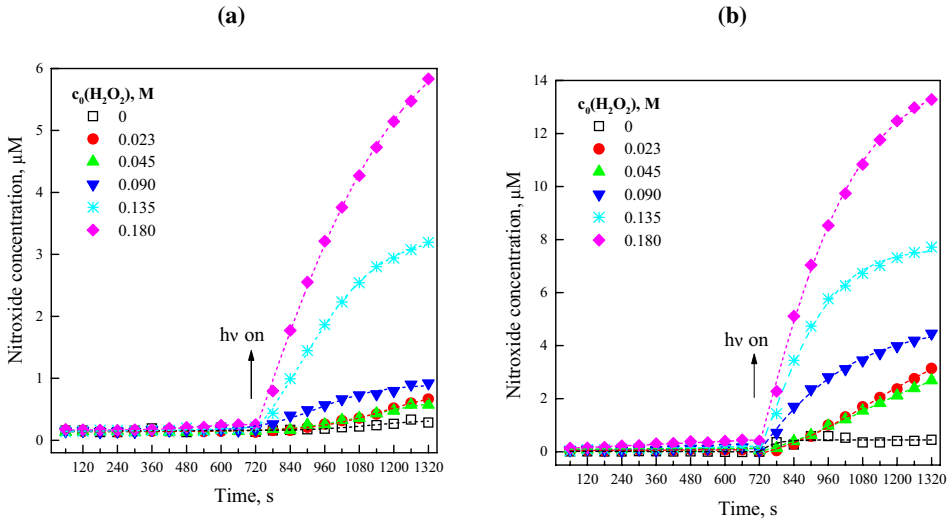

Figure 5. Time dependence of the concentration of nitroxide produced *via* TMP oxidation in acetonitrile solutions containing various initial concentration of H_2O_2 monitored in the dark and on continuous irradiation: (a) under air; (b) under argon. Initial concentration: c_0(TMP) = 0.01 M; irradiation wavelength 365 nm. The symbols represent the experimental data and the dashed lines their mathematical simulations using least squares analysis.

Consequently, if hydroxyl radicals cause oxidation of TMP to nitroxide radicals, competitive reactions with DMSO should result in a decrease of the nitroxide concentration. In reality, the addition of DMSO significantly hindered the generation of nitroxides, specifically there was a 90% decrease of a signal, which is attributable to nitroxide after 600 s of exposure (Fig. 6), and these findings support the hypothesis that TMP may be oxidized to nitroxides not only *via* singlet oxygen but also *via* photogenerated hydroxyl radicals.

The results of EPR spin trapping experiments in solutions of H_2O_2/DMPO/ACN/argon after 600 s exposure evidenced the presence of $^{\bullet}$DMPO-O_2^{-}/OOH and $^{\bullet}$DMPO-OH (Fig. 7a) and no carbon-centered spin adducts were found. Under the given experimental conditions, the photogenerated hydroxyls radicals are either added to DMPO, or react with hydrogen peroxide (Eqs. [7] and [8]) producing $O_2^{\bullet-}$/$^{\bullet}$OOH species, trapped as corresponding DMPO spin adducts. However, the addition of DMSO, which behaves as an effective hydroxyl radical scavenger, into the solution H_2O_2/DMPO/ACN/argon resulted upon irradiation in the generation of the spin adducts $^{\bullet}$DMPO-O_2^{-} and $^{\bullet}$DMPO-OH, along with spin adducts originating from the reaction of DMSO with $^{\bullet}$OH, *i.e.* $^{\bullet}$DMPO-CH_3 (a_N = 1.479 mT, a_H^{β} = 2.118 mT; g = 2.0057) and $^{\bullet}$DMPO-OCH_3 (a_N = 1.331 mT, a_H^{β} = 0.802 mT, a_H^{γ} = 0.172 mT; g = 2.0059). We propose that $^{\bullet}$DMPO-OCH_3 is produced in the reaction of methyl radicals with molecular oxygen as was published previously (5,59,60).

Oxidation of TMP and TMPO in acetonitrile titanium dioxide suspensions

The photoexcitation of titanium dioxide in acetonitrile suspensions leads to the simultaneous generation of superoxide radical anion, singlet oxygen, hydrogen peroxide and hydroxyl radicals. It is obvious that on the TiO_2 surface are bound hydroxyl groups and water molecules (3,61), which act as acceptors of photogenerated holes and produce hydroxyl radicals (62), thus the presence of small amounts of water

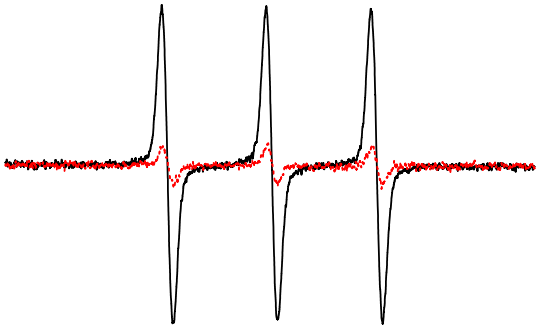

Figure 6. Experimental EPR spectra (SW = 8 mT) measured after 600 s irradiation of TMP in the presence of H_2O_2 in deoxygenated acetonitrile (solid line) or mixed solvent ACN/DMSO (DMSO 20%; vol; dotted line). Initial concentrations: $c_0(H_2O_2)$ = 0.135 M, c_0(TMP) = 0.01 M; irradiation wavelength 365 nm.

cannot be excluded even if dried ACN is used for the suspensions preparation. The above mentioned experiments performed in homogeneous solutions show the impact of water presence in acetonitrile on the behavior of the superoxide radical anions (Fig. 3). Therefore, TMP or TMPO are not appropriate agents to selectively monitor the photoinduced formation of singlet oxygen, since the generation of nitroxide radicals could also result from the reactions of SHA with other ROS generated upon exposure of TiO_2 particulate systems. Furthermore, upon the irradiation of titania in the presence of SHA, the nitroxide radicals may be generated *via* the direct oxidation by the photogenerated holes (18).

The detailed study of the oxidation of 2,2,6,6-tetrametylpiperidine derivatives in aqueous TiO_2 suspensions was published previously using titania loadings up to 6 g L^{-1} along with high TMP concentrations (0.1–0.5 M; 18). The supposed reaction mechanism involves the oxidation of SHA with photogenerated holes producing unstable intermediates, which react with oxygen to form nitroxide radicals; the oxidation of SHA *via* singlet oxygen, superoxide radical anions or hydroxyl radicals was excluded.

On the other hand, in recently published articles (9,51) the UV irradiation of aqueous suspensions of TiO_2 containing SHA failed to generate nitroxide radicals. However, our attempts to evidence the photoinduced oxidation of SHA upon irradiation of titania in the presence of TMP or TMPO were not successful in H_2O or D_2O solvents under air, probably due to considerably lower TiO_2 and SHA concentrations as applied in (18). In accord with the recommendations of reviewers we performed an additional set of EPR experiments with TMP and TMPO in aqueous titania suspensions, in which we confirmed the substantial role of initial molecular oxygen concentration dissolved in the heterogeneous system filled in the EPR flat cell. In the TiO_2 suspensions (0.4 g L^{-1}) containing TMP or TMPO (c_0 = 0.01 M) carefully saturated with oxygen we observed on continuous irradiation (λ = 365 nm) a set of EPR spectra revealing the progressive increase of nitroxide concentration without decline upon 600 s exposure.

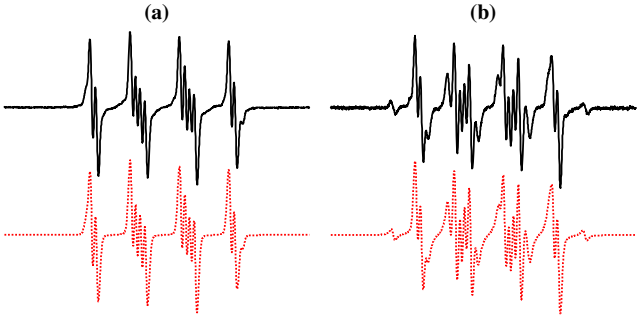

Figure 7. Experimental (solid line) and simulated (dotted line) EPR spectra (SW = 8 mT) obtained after 600 s irradiation of the deoxygenated solutions of H_2O_2 in the presence of the DMPO spin trap: (a) acetonitrile; (b) mixed solvent ACN/DMSO (DMSO 20%; vol). Initial concentrations: $c_0(H_2O_2)$ = 0.135 M, c_0(DMPO) = 0.04 M; irradiation wavelength 365 nm. Simulation parameters: (a) •DMPO-O_2^-/OOH (a_N = 1.299 mT, a_H^{β} = 1.051 mT, a_H^{γ} = 0.127 mT; g = 2.0059; 89%), •DMPO-OH (a_N = 1.378 mT, a_H^{β} = 1.210 mT, a_H^{γ} = 0.086 mT; g = 2.0059; 11%); (b) •DMPO-O_2^- (a_N = 1.293 mT, a_H^{β} = 1.030 mT, a_H^{γ} = 0.137 mT; g = 2.0059; 35%), •DMPO-OCH_3 (a_N = 1.331 mT, a_H^{β} = 0.802 mT, a_H^{γ} = 0.172 mT; g = 2.0059; 49%); •DMPO-CH_3 (a_N = 1.479 mT, a_H^{β} = 2.118 mT; g = 2.0057; 11%); •DMPO-OH (5%).

In the aerated acetonitrile TiO_2 suspensions the continuous exposure resulted in the gradual growth of a three-line EPR signal attributable to nitroxide radicals as shown in Fig. 8. The presence of titania is cardinal, as in the titania-free TMP or TMPO acetonitrile solutions the photoinduced generation of nitroxide radicals is negligible (Fig. 8a,b). Increase in the TiO_2 concentration causes a substantial increase in the nitroxide radical concentration formed upon irradiation, up to a titania loading of 0.4 g L^{-1}, at which point a limitation in the initial rate of nitroxide formation is observed and with even higher concentrations of TiO_2 the concentration of paramagnetic nitroxide species decreases upon prolonged irradiation (Fig. 8), most probably due to the termination reactions with ROS generated in TiO_2 system (37–39,63).

In the photoinduced reactions in TiO_2 systems, molecular oxygen plays a very important role because it acts as an electron acceptor, providing an effective separation of photogenerated charge carriers and so prevents their recombination. Due to the reaction of molecular oxygen with the photogenerated electrons the concentration of dissolved molecular oxygen in the experimental TiO_2 systems decreases on continuous irradiation (64), and such a decline can be easily monitored by EPR spectroscopy by measuring the peak-to-peak line widths (ΔB_{pp}) in the EPR spectra of the nitroxides. Upon the exposure of TiO_2 acetonitrile suspensions in the presence of SHA under the given experimental conditions, we observed an exponential decrease in ΔB_{pp} during continuous irradiation, which was accelerated with the growth of titania loading (data not shown).

To obtain more information on the reaction mechanisms of SHA reactions with ROS in the photocatalytic systems, we performed a set of experiments in TiO_2 suspensions containing invariant concentrations of TiO_2 and SHA, and a variable initial

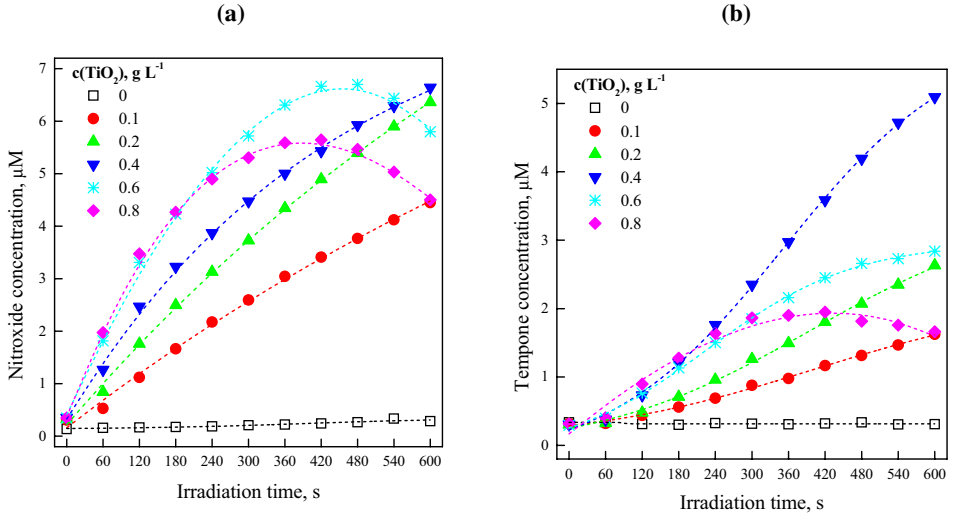

Figure 8. Time dependence of the paramagnetic species concentration produced *via* hindered amines oxidation on continuous irradiation under air in acetonitrile titanium dioxide suspensions containing various TiO_2 loadings in the presence of: (a) TMP; (b) TMPO. Initial concentrations: c_0(TMP) = 0.01 M, c_0(TMPO) = 0.01 M; irradiation wavelength 365 nm. The symbols represent the experimental data and the dashed lines their mathematical simulations using least squares analysis.

concentration of BHT, which behaves as an effective singlet oxygen quencher (65). Addition of BHT, even at low concentrations (40 μM), caused a significant decrease in TMP and TMPO oxidation (data not shown). However, the results obtained require very careful interpretation as BHT can terminate not only singlet oxygen but also other ROS generated (65). Thus, the decline in nitroxide concentration monitored during photoexcitation of TiO_2/SHA/BHT/acetonitrile/air systems cannot be attributed to a selective interaction of BHT with singlet oxygen, but also to the parallel reactions with different ROS photogenerated in TiO_2 suspensions.

The reactions of charge carriers and reactive species photogenerated upon irradiation in TiO_2/acetonitrile suspensions are strongly influenced by the presence of substances acting as electron acceptors/donors or reacting with hydroxyl radicals or singlet oxygen. Consequently, we studied the oxidation of TMPO in aerated acetonitrile titania suspensions containing as a cosolvent (4%; vol): (1) water (h^+ acceptor, source of $^\bullet OH$, reacts with $O_2^{\bullet-}$), (2) DMSO ($^\bullet OH$ quencher), (3) methanol (h^+ acceptor, $^\bullet OH$ quencher) and (4) water with NaN_3 (singlet oxygen and $^\bullet OH$ quencher). The concentration of Tempone found in these systems after 600 s of irradiation is summarized in Fig. 9. The experiments in titania ACN suspensions with added water (Fig. 9) were performed with the aim to obtain a correct reference for the effect of sodium azide, because the stock solution of this reagent was prepared in water (low solubility in ACN), which was mixed with acetonitrile to obtain suspension containing 4% of water in ACN and 0.004 M of NaN_3 (Fig. 9). While the addition of 4% water caused about 13% decrease in nitroxide concentration in comparison with pristine system TiO_2/TMPO/acetonitrile/air, a substantial decrease (60%) was found in the analogous system containing NaN_3, as well as in a TiO_2 slurry prepared with DMSO. The highest (92%) reduction of TMPO oxidation was found in the presence of methanol, which reacts competitively with photogenerated holes and hydroxyl radicals, and inhibits the possible oxidation of TMPO *via* holes, singlet oxygen, as well as hydroxyl radicals.

In addition, the generation of unstable paramagnetic intermediates in the above experimental photocatalytic systems was examined by the EPR spin trapping technique, using DMPO as spin trap at an identical initial concentration as for TMPO ($c_{0,DMPO} = c_{0,TMPO} = 0.01$ M). The photoexcitation and photoinduced generation of paramagnetic species was performed under aerobic conditions in the presence of molecular oxygen, which serves as an electron acceptor. Therefore, the EPR spectra obtained upon *in situ* irradiation are characterized by broad spectral lines as illustrates Fig. 10a. To obtain EPR spectra sufficiently well resolved for a detailed simulation analysis, the suspensions, after 600 s exposure in the EPR resonator, were rapidly saturated with argon, immediately replaced into the EPR cell, reinserted into the cavity and EPR spectra were measured again under inert atmosphere without further exposure (Fig. 10b). The EPR spectra found in TiO_2/TMPO/DMPO/ACN are attributed to $^\bullet$DMPO-O_2^- (64%), $^\bullet$DMPO-OCH_3 (28%) and Tempone (8%). The irradiation of TiO_2/TMPO/DMPO/NaN_3/ACN/water results in the generation of spin adducts unambiguously assigned to $^\bullet$DMPO-N_3^- ($a_{N(NO)} = 1.350$ mT, $a_H^\beta = 1.232$ mT, $a_N = 0.316$ mT; $g = 2.0059$; 98%) and Tempone (2%). Sodium azide is a frequently used $^1O_2$ inhibitor (22), but it

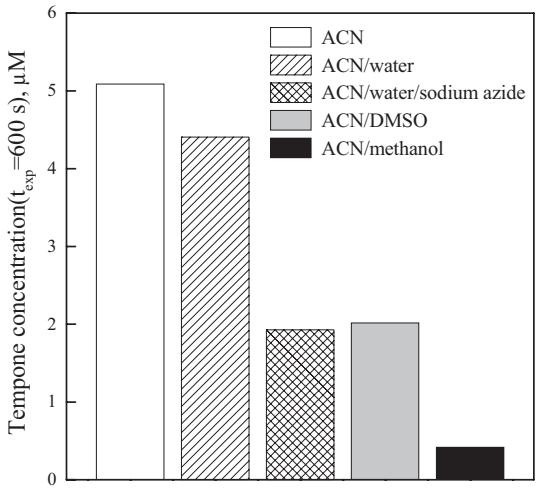

Figure 9. Tempone concentration monitored after 600 s of irradiation in aerated TiO_2 suspensions containing TMPO in acetonitrile or mixed solvents as specified in legend (cosolvent 4%; vol). Initial concentrations: $c(TiO_2) = 0.4$ g L^{-1}, $c_0(TMPO) = 0.01$ M, $c_0(NaN_3) = 0.004$ M; irradiation wavelength 365 nm.

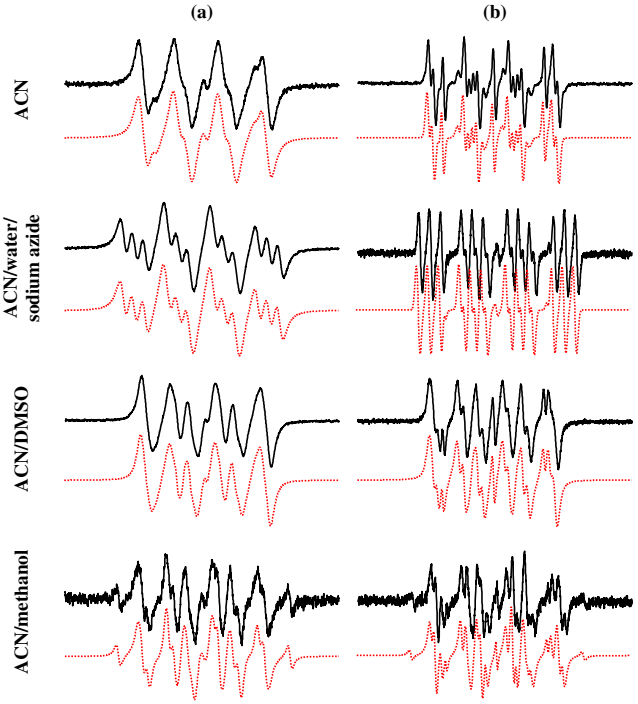

Figure 10. Experimental (solid line) and simulated (dotted line) EPR spectra (SW = 8 mT) obtained after 600 s exposure in TiO_2 suspensions containing TMPO and DMPO in acetonitrile or mixed solvents as specified in legends (cosolvent 4%; vol): (a) under air immediately after irradiation, irradiation wavelength 365 nm; (b) as (a) after subsequent saturation with argon. Initial concentrations: $c(TiO_2) = 0.4$ g L^{-1}, $c_0(TMPO) = 0.01$ M, $c_0(DMPO) = 0.04$ M, $c_0(NaN_3) = 0.004$ M. Simulation parameters for EPR spectra shown in (b): *ACN*: $^\bullet$DMPO-O_2^- (64%), $^\bullet$DMPO-OCH_3 (28%), Tempone (8%); *ACN/water/sodium azide*: $^\bullet$DMPO-N_3^- ($a_{N(NO)} = 1.350$ mT, $a_H^\beta = 1.232$ mT, $a_N = 0.316$ mT; $g = 2.0059$; 98%), Tempone (2%). *ACN/DMSO*: $^\bullet$DMPO-O_2^- (10%), $^\bullet$DMPO-OCH_3 (85%), Tempone (5%); *ACN/methanol*: $^\bullet$DMPO-O_2^- (51%), $^\bullet$DMPO-OCH_3 (43%), $^\bullet$DMPO-CR′ ($a_N = 1.479$ mT, $a_H^\beta = 2.099$ mT; $g = 2.0057$; 4%), Tempone (2%).

interacts also with hydroxyl radicals producing $N_3^{\bullet-}$ (6,40). However, the direct oxidation of azide with the photogenerated holes represents a far more plausible alternative of $N_3^{\bullet-}$ generation.

The experimental EPR spectra obtained in the system TiO_2/TMPO/DMPO/ACN/DMSO corresponded to the generation of $^{\bullet}DMPO\text{-}O_2^-$ (10%), $^{\bullet}DMPO\text{-}OCH_3$ (85%) and Tempone (5%), but in the presence of methanol, in addition to $^{\bullet}DMPO\text{-}O_2^-$ (51%) $^{\bullet}DMPO\text{-}OCH_3$ (43%) and Tempone (2%), a carbon-centered spin adduct $^{\bullet}DMPO\text{-}CR'$ (a_N = 1.479 mT, a_H^{β} = 2.099 mT; g = 2.0057; 4%) was also found (Fig. 10). In good correlation with the mechanism of titania particle photoactivation under aerobic conditions, EPR spin trapping experiments confirmed the generation of superoxide radical anions, hydroxyl radicals, and further radical species originating from the interaction with solvents. Therefore, it is necessary to assume that TMPO may be oxidized to Tempone *via* alternative mechanisms including $^1O_2$, hydroxyl radicals or direct electron transfer to photo-excited TiO_2.

Oxidation of TMP and TMPO in acetonitrile titanium dioxide suspensions in the presence of H_2O_2

Continuous photoexcitation of TiO_2/TMPO/ACN/H_2O_2/air or TiO_2/TMPO/ACN/H_2O_2/argon was monitored to obtain information on the impact of hydrogen peroxide on the oxidation of TMPO to Tempone, as H_2O_2 behaves as effective acceptor of both photogenerated charge carriers (66; Eqs. [14] and [15]):

$$H_2O_2 + e^- \rightarrow {}^{\bullet}OH + OH^- \quad (14)$$

$$H_2O_2 + h^+ \rightarrow {}^{\bullet}OOH + H^+ \quad (15)$$

However, hydroxyl and hydridodioxygen radicals can be produced simultaneously *via* the processes summarized in Eqs. [7]–[11].

Figure 11a,b shows the photoinduced generation of Tempone in the titania suspensions with added hydrogen peroxide under air or argon, along with the reference systems without H_2O_2. The results of reference experiments confirm the significant role of

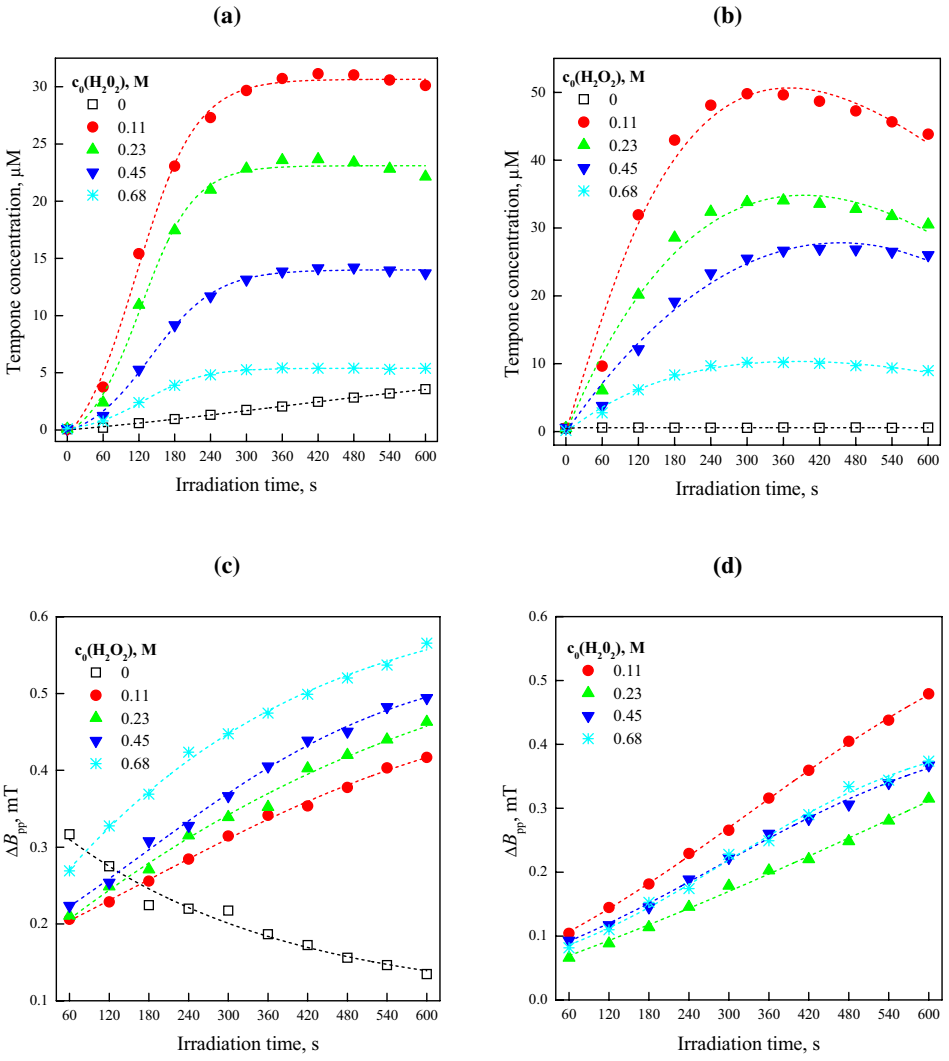

Figure 11. Time dependence of the Tempone concentration produced *via* TMPO oxidation on continuous irradiation in acetonitrile titanium dioxide suspensions containing various initial concentrations of H_2O_2, along with changes in peak-to-peak line width of EPR spectra (ΔB_{pp}): (a, c) under air; (b, d) under argon. Initial concentrations: c_0(TMPO) = 0.01 M, c(TiO_2) = 0.4 g L^{-1}; irradiation wavelength 365 nm. The symbols represent the experimental data and the dashed lines their mathematical simulations using least squares analysis.

molecular oxygen in the charge separation processes on irradiated TiO_2 as, under argon, the oxidation of TMPO is fully inhibited (Fig. 11b). The addition of H_2O_2 at the lowest concentration used in our study (c_0 = 0.11 M) substantially increases the concentration of Tempone generated upon exposure, however, further increase in hydrogen peroxide in the systems causes the reverse effect (Fig. 11a,b). The prolonged irradiation of suspensions containing H_2O_2 leads to the decomposition of nitroxide, especially in the systems saturated with argon before irradiation (Fig. 11b).

To confirm that the presence of hydrogen peroxide significantly increases the degradation of Tempone, additional experiments were performed, in which Tempone was irradiated in TiO_2 suspensions without/with added H_2O_2 (Fig. 12). Under the given experimental conditions the decrease in Tempone concentration is significantly accelerated by the addition of H_2O_2 (Fig. 12). Irradiation of nitroxide radicals in TiO_2 suspensions results in the termination of paramagnetic $>NO^{\bullet}$ group *via* electron transfer or the reactions with ROS, and the decline in EPR signal intensity was successfully used previously for the determination TiO_2 photocatalysts activity (12).

An important fact we observed under air or inert atmosphere during the irradiation of the systems TiO_2/TMPO /ACN/H_2O_2 is a significant enlargement of the peak-to-peak line widths in EPR spectra of Tempone (Fig. 11c,d), which clearly demonstrates the formation of molecular oxygen during photoinduced reaction of H_2O_2 in TiO_2 suspensions. Triplet molecular oxygen can be formed by the reactions of hydrogen peroxide with hydridodioxygen radical (Eq. [10]) or by mutual termination of $^{\bullet}OOH$ radicals (Eq. [11]), but in this case the singlet state of the oxygen generated cannot be excluded (47). In accordance with the previous results in titania suspensions without H_2O_2 addition, the peak-to-peak line widths of Tempone reveal reverse behavior upon exposure (Fig. 11c; open squares), which is consistent with the decrease in the concentration of dissolved molecular oxygen due to the reaction with photogenerated electrons.

The results obtained in the oxidation of TMP under analogous conditions are consistent with the results observed for Tempone generation from TMPO. Also here we observed the highest concentration of nitroxide radicals in suspensions with the lowest initial concentration of hydrogen peroxide (c_0 = 0.11 M) in both atmospheres (data not shown) and a further increase of the initial H_2O_2 concentration inhibited the nitroxide formation. Under an inert atmosphere without the addition of H_2O_2 oxidation of TMP does not take place as the system lacks an electron acceptor. The changes in the peak-to-peak line widths of nitroxide radicals monitored in systems TiO_2/TMP/ACN/H_2O_2/air and TiO_2/TMP/ACN/H_2O_2 /argon were fully compatible with data shown in Fig. 11c,d.

The photoinduced reactions of SHA in titania suspensions with added H_2O_2 represent a complex system in which the photogenerated species with a high oxidative potential (h^+, $^{\bullet}OH$, $^1O_2$) cause not only generation of nitroxide radicals but also their consecutive transformation into diamagnetic products.

Oxidation of TMP and TMPO in acetonitrile titanium dioxide suspensions in the presence of KO_2

The formation of superoxide radical anions in the irradiated TiO_2 suspensions results from the effective capture of photogenerated electrons by molecular oxygen (3). We were interested in how the addition of KO_2 into the photocatalytic systems TiO_2/SHA/ACN/air and TiO_2/SHA/ACN/argon will affect the oxidation of cyclic amines to nitroxide radicals. The presence of KO_2 in suspensions of TiO_2/TMPO/ACN/air leads to a growth in the initial rate of Tempone generation upon irradiation, but prolonged exposure in the systems with higher KO_2 concentrations causes a decrease in the nitroxide concentration (Fig. 13a). This decline most probably reflects the termination of $>NO^{\bullet}$ in the reactions with holes, $O_2^{\bullet-}$ or singlet oxygen.

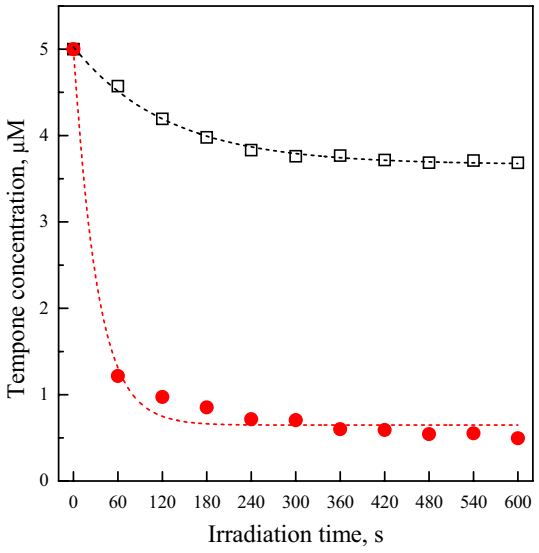

Figure 12. Time dependence of Tempone concentration monitored on continuous irradiation in acetonitrile titanium dioxide suspensions under air without (□) and in the presence of H_2O_2 (●). Initial concentrations: c_0(Tempone) = 5 μM, c(TiO_2) = 0.4 g L^{-1}, c_0(H_2O_2) = 0.11 M; irradiation wavelength 365 nm. The symbols represent the experimental data and the dashed lines their mathematical simulations using least squares analysis of a first-order kinetic model.

During the photoinduced reactions in these systems the peak-to-peak line widths decrease (data not shown), evidencing a decrease in the concentration of dissolved molecular oxygen. The results of the experiments in homogeneous acetonitrile solutions (Fig. 3) along with the literature data (26) show that in anhydrous aprotic media superoxide radical anions do not react with TMPO. We assume that the superoxide radical anions, added as KO_2 into the titania suspensions under the given experimental conditions, interact with photogenerated holes producing singlet oxygen, which oxidize TMPO to Tempone. On the other hand, we cannot exclude the presence of low concentrations of hydrogen peroxide and hydroxyl radicals, as potential alternative oxidants of TMPO.

Oxidation of TMPO to paramagnetic Tempone in TiO_2/TMPO/ACN/KO_2/argon suspensions during UVA radiation (λ = 365 nm) photoexcitation does not take place because the system lacks a suitable electron acceptor to inhibit the recombination of photogenerated charge carriers. After the addition of Ag^+ ions, which are able to act as efficient electron acceptors (66), in the deaerated TiO_2 suspensions containing KO_2 the instantaneous generation of Tempone is observed, and its concentration gradually increases until reaching a

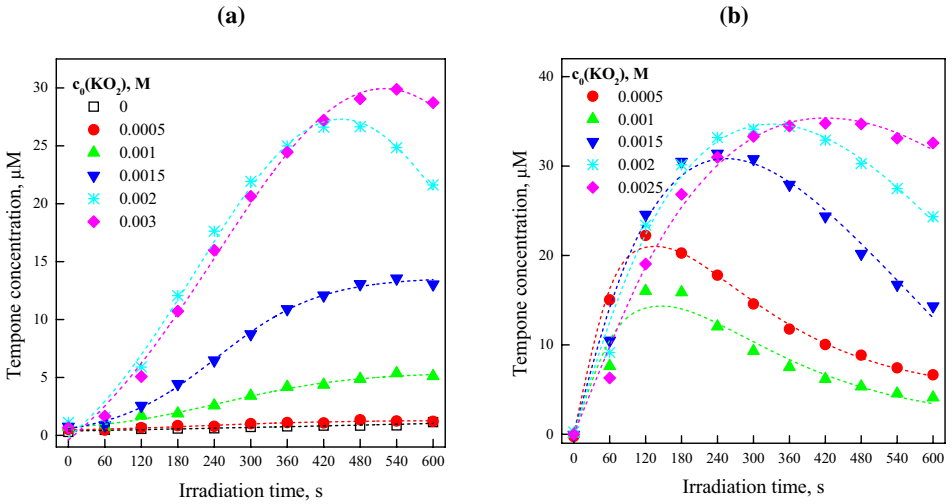

Figure 13. Time dependence of the Tempone concentration produced *via* TMPO oxidation on continuous irradiation in acetonitrile titanium dioxide suspensions containing various initial concentrations of KO_2: (a) under air; (b) under argon with addition of $AgNO_3$. Initial concentrations: c_0(TMPO) = 0.01 M, $c(TiO_2)$ = 0.4 g L^{-1}, $c_0(AgNO_3)$ = 0.01 M; irradiation wavelength 365 nm. The symbols represent the experimental data and the dashed lines their mathematical simulations using least squares analysis.

maximum and then decreases (Fig. 13b). The photoexcitation of titania leads to the reduction of Ag^+ ions to elemental silver deposited on the surface of titanium dioxide, which is noticeable as a change in color of the photocatalyst. The results obtained in the oxidation of TMP under analogous conditions are in good correlation with data found upon TMPO oxidation.

CONCLUSIONS

The EPR investigations in our study were focussed on the oxidation of TMP and TMPO to nitroxide radicals during exposure with monochromatic UVA radiation (λ = 365 nm) in acetonitrile solutions and titanium dioxide suspensions. Despite of high potential of EPR spectroscopy in the characterization of paramagnetic species, the experimental techniques applied (oxidation of SHA to nitroxide radicals and spin trapping) represent indirect methods, and the results obtained require careful interpretation due to the complexity and interconnection of ROS reactions in studied systems. We suggested the alternative reactions pathways leading to singlet oxygen and other ROS generation in the investigated systems, and their role in the TMP and TMPO oxidation in dark, as well as upon UVA exposure (λ = 365 nm). The reactions of SHA with oxidative species considered in our study are schematically summarized in Scheme 1 (The Radziszewski

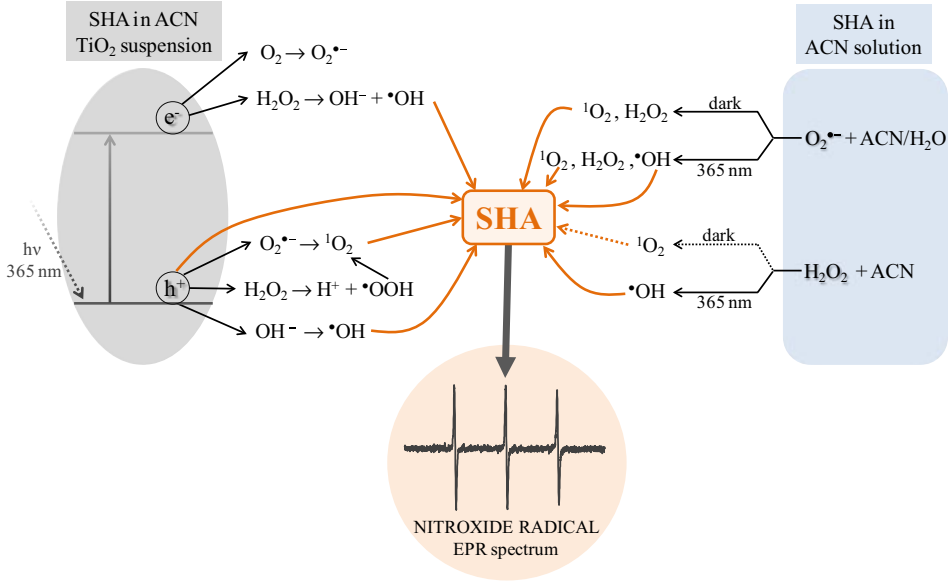

Scheme 1. Schematic summarization of SHA oxidation to nitroxide radicals *via* oxidative species considered in the investigations in acetonitrile solutions and titania suspensions on monochromatic 365 nm irradiation (the Radziszewski reaction of H_2O_2 with acetonitrile in dark was negligible under the experimental conditions used in our study, so this reaction pathway is shown with dotted lines and arrow. Hydrogen peroxide concentration range: 0.023–0.68 M).

reaction of H_2O_2 with acetonitrile in dark was negligible under the experimental conditions used in our study, so this reaction pathway is shown with dotted lines and arrow).

The results of EPR experiments performed in our study can be summarized as follows: In acetonitrile solutions TMP and TMPO are oxidized to nitroxide radicals *via* (1) singlet oxygen generated for example by the excitation of the dye Eosin Y and (2) hydrogen peroxide and hydroxyl radicals generated by H_2O_2 photolysis in acetonitrile solutions. The oxidation of TMP can produce not only Tempol (oxidation of the >NH group) but also Tempone *via* subsequent oxidation of the 4-hydroxy group.

In anhydrous acetonitrile solutions TMP and TMPO do not react with KO_2, but the addition of water to the systems results in SHA oxidation due to the generation of singlet oxygen (without irradiation); however, the irradiation caused a significant increase in the nitroxide concentration.

In the irradiated acetonitrile TiO_2 suspensions the oxidation of TMP and TMPO can take place due the reaction with singlet oxygen, hydrogen peroxide, hydroxyl radicals or photogenerated holes. EPR spin trapping experiments using DMSO and methanol as cosolvents confirmed the participation of hydroxyl radicals in the generation of nitroxide radicals. In the presence of superoxide radical anions added into TiO_2 suspensions as KO_2, the oxidation of TMP and TMPO occurs also under an inert atmosphere in the presence of a suitable acceptor of photogenerated electrons (*e.g.* Ag^+ ions); most probably *via* singlet oxygen originating from the reaction of photogenerated holes with the superoxide radical anions.

Acknowledgements—This study was financially supported by Scientific Grant Agency (VEGA project 1/0289/12). Harry Morris is gratefully acknowledged for helpful discussion.

REFERENCES

1. Wang, Z., W. Ma, C. Chen, H. Ji and J. Zhao (2011) Probing paramagnetic species in titania-based heterogeneous photocatalysis by electron spin resonance (ESR) spectroscopy—A mini review. *Chem. Eng. J.* **170**, 353–362.
2. Fujishima, A., X. Zhang and D. Tryk (2008) TiO_2 photocatalysis and related surface phenomena. *Surf. Sci. Reports* **63**, 515–582.
3. Henderson, M. (2011) A surface science perspective on TiO_2 photocatalysis. *Surf. Sci. Reports* **66**, 185–297.
4. Ohtani, B. (2010) Photocatalysis A to Z—What we know and what we do not know in a scientific sense. *J. Photochem. Photobiol. C: Photochem. Rev.* **11**, 157–178.
5. Brezová, V., S. Gabčová, D. Dvoranová and A. Staško (2005) Reactive oxygen species produced upon photoexcitation of sunscreens containing titanium dioxide (an EPR study). *J. Photochem. Photobiol. B: Biol.* **79**, 121–134.
6. Janczyk, A., A. Wolnicka-Gtubisz, K. Urbanska, H. Kisch, G. Stochel and W. Macyk (2008) Photodynamic activity of platinum(IV) chloride surface-modified TiO_2 irradiated with visible light. *Free Radic. Biol. Med.* **44**, 1120–1130.
7. Buchalska, M., G. Kras, M. Oszajca, W. Lasocha and W. Macyk (2010) Singlet oxygen generation in the presence of titanium dioxide materials used as sunscreens in suntan lotions. *J. Photochem. Photobiol. A: Chem.* **213**, 158–163.
8. Macyk, W., A. Franke and G. Stochel (2005) Metal compounds and small molecules activation—Case studies. *Coord. Chem. Rev.* **249**, 2437–2457.
9. Lipovsky, A., L. Levitski, Z. Tzitrinovich, A. Gedanken and R. Lubart (2012) The different behavior of rutile and anatase nanoparticles in forming oxy radicals upon illumination with visible light: An EPR study. *Photochem. Photobiol.* **88**, 14–20.
10. Carp, O., C. Huisman and A. Reller (2004) Photoinduced reactivity of titanium dioxide. *Prog. Solid State Chem.* **32**, 33–177.
11. Ahmed, S., M. Rasul, W. Martens, R. Brown and M. Hashib (2011) Advances in heterogeneous photocatalytic degradation of phenols and dyes in wastewater: A review. *Water Air Soil Pollut.* **215**, 3–29.
12. Brezová, V., D. Dvoranová and A. Staško (2007) Characterization of titanium dioxide photoactivity following the formation of radicals by EPR spectroscopy. *Res. Chem. Intermed.* **33**, 251–268.
13. Wu, H., Q. Song, G. Ran, X. Lu and B. Xu (2011) Recent developments in the detection of singlet oxygen with molecular spectroscopic methods. *Trends Anal. Chem.* **30**, 133–141.
14. Konaka, R., E. Kasahara, W. Dunlap, Y. Yamamoto, K. Chien and M. Inoue (1999) Irradiation of titanium dioxide generates both singlet oxygen and superoxide anion. *Free Radic. Biol. Med.* **27**, 294–300.
15. Daimon, T., T. Hirakawa, M. Kitazawa, J. Suetake and Y. Nosaka (2008) Formation of singlet molecular oxygen associated with the formation of superoxide radicals in aqueous suspensions of TiO_2 photocatalysts. *Appl. Catal. A: Gen.* **340**, 169–175.
16. Lion, Y., M. Delmelle and A. Van De Vorst (1976) New method of detecting singlet oxygen production. *Nature* **263**, 442–443.
17. Rosenthal, I., C. Krishna, G. Yang, T. Kondo and P. Riesz (1987) A new approach for EPR detection of hydroxyl radicals by reaction with sterically hindered cyclic amines and oxygen. *FEBS Lett.* **222**, 75–78.
18. Nosaka, Y., H. Natsui, M. Sasagawa and A. Nosaka (2006) Electron spin resonance studies on the oxidation mechanism of sterically hindered cyclic amines in TiO_2 photocatalytic systems. *J. Phys. Chem. B* **110**, 12993–12999.
19. Barbieriková, Z., M. Bella, J. Kučerák, V. Milata, S. Jantová, D. Dvoranová, M. Veselá, A. Staško and V. Brezová (2011) Photoinduced superoxide radical anion and singlet oxygen generation in the presence of novel selenadiazoloquinolones (an EPR study). *Photochem. Photobiol.* **87**, 32–44.
20. Barbieriková, Z., M. Bella, J. Lietava, D. Dvoranová, A. Staško, T. Füzik, V. Milata, S. Jantová and V. Brezová (2011) Spectroscopic characterization and photoinduced processes of 4-oxoquinoline derivatives. *J. Photochem. Photobiol. A: Chem.* **224**, 123–134.
21. Banerjee, D., P. Kumar, B. Kumar, U. Madhusoodanan, S. Nayak and J. Jacob (2002) Determination of absolute hydrogen peroxide concentration by spectrophotometric method. *Curr. Sci.* **83**, 1193–1194.
22. NIEHS (2002) *WinSIM*, NIEHS, Research Triangle Park, NC. Available at: http://www.niehs.nih.gov/research/resources/software/tox-pharm/tools/index.cfm. Accessed on 24 April 2012.
23. Li, M., C. Cline, E. Koker, H. Carmichael, C. Chignell and P. Bilski (2001) Quenching of singlet molecular oxygen ($^1O_2$) by azide anion in solvent mixtures. *Photochem. Photobiol.* **74**, 760–764.
24. Braun, A. M., M.-T. Maurette and E. Oliveros (1986) *Technologie Photochimique*. Presses Polytechniques Romandes, Lausanne, 442–443.
25. Wadhawan, J., P. Welford, H. McPeak, C. Hahn and R. Compton (2003) The simultaneous voltammetric determination and detection of oxygen and carbon dioxide—A study of the kinetics of the reaction between superoxide and carbon dioxide in non-aqueous media using membrane-free gold disc microelectrodes. *Sens. Actuators B: Chem.* **88**, 40–52.
26. Zang, L., F. vanKuijk, B. Misra and H. Misra (1995) The specificity and product of quenching singlet oxygen by 2,2,6,6-tetramethylpiperidine. *Biochem. Mol. Biol. Int.* **37**, 283–293.
27. Lion, Y., E. Gandin and A. Van de Vorst (1980) On the production of nitroxide radicals by singlet oxygen reaction: An EPR study. *Photochem. Photobiol.* **31**, 305–309.
28. Ciba-Geigy Corporation, Pastor, S. D., A. R. Smith and K. M. Bessonen (1997) Hydrogen Peroxide Oxidation of 4-Hydroxy-2,2,6,6,-Tetramethylpiperidine. US Patent: 5,654,434, 5 August

1997. Available at: http://patents.justia.com/1997/05654434.html. Accessed on 24 April 2012.
29. Brezová, V., P. Billik, Z. Vrecková and G. Plesch (2010) Photoinduced formation of reactive oxygen species in suspensions of titania mechanochemically synthesized from $TiCl_4$. *J. Mol. Catal. A: Chem.* **327**, 101–109.
30. Poupko, R. and I. Rosenthal (1973) Electron transfer interactions between superoxide ion and organic compounds. *J. Phys. Chem.* **77**, 1722–1724.
31. Li, A., K. Cummings, H. Roethling, G. Buettner and C. Chignell (1988) A spin-trapping database implemented on the IBM PC/AT. *J. Magn. Reson.* **79**, 140–142. Available at: http://mole.chm.bris.ac.uk/cgi-bin/stdb. Accessed on 24 April 2012.
32. Cervera, M. and J. Marquet (1998) Effects of superoxide anion generated from aromatic radical anions produced in nucleophilic aromatic photosubstitution reactions. *Can. J. Chem.* **76**, 966–969.
33. Gibian, M. J., D. T. Sawyer, T. Ungermann, R. Tangpoonpholvivat and M. M. Morrison (1979) Reactivity of superoxide ion with carbonyl compounds in aprotic solvents. *J. Am. Chem. Soc.* **101**, 640–644.
34. Corey, E., M. Mehrotra and A. Khan (1987) Water induced dismutation of superoxide anion generates singlet molecular-oxygen. *Biochem. Biophys. Res. Commun.* **145**, 842–846.
35. Sawyer, D. T. and J. S. Valentine (1981) How super is superoxide? *Acc. Chem. Res.* **14**, 393–400.
36. Wilkinson, F., W. Helman and A. Ross (1995) Rate constants for the decay and reactions of the lowest electronically excited singlet-state of molecular-oxygen in solution—An expanded and revised compilation. *J. Phys. Chem. Ref. Data* **24**, 663–1021.
37. Martinez, C., S. Jockusch, M. Ruzzi, E. Sartori, A. Moscatelli, N. Turro and A. Buchachenko (2005) Chemically induced dynamic electron polarization generated through the interaction between singlet molecular oxygen and nitroxide radicals. *J. Phys. Chem. A* **109**, 10216–10221.
38. Vidoczy, T. and P. Baranyai (2001) Quenching of porphyrin triplet and singlet oxygen by stable nitroxide radicals: Importance of steric hindrance. *Helv. Chim. Acta* **84**, 2640–2652.
39. Glebska, J., L. Pulaski, K. Gwozdzinski and J. Skolimowski (2001) Structure-activity relationship studies of protective function of nitroxides in Fenton system. *Biometals* **14**, 159–170.
40. Halliwel, B. and J. Gutteridge (1999) *Free Radicals in Biology and Medicine*, 3rd edn. Oxford University Press, New York, NY, Oxford.
41. Brauer, H., B. Eilers and A. Lange (2002) Formation of singlet molecular oxygen by the Radziszewski reaction between acetonitrile and hydrogen peroxide in the absence and presence of ketones. *J. Chem. Soc., Perkin Trans. 2*, 1288–1295.
42. Gugumus, F. (1993) Current trends in mode of action of hindered amine light stabilizers. *Polym. Degrad. Stab.* **40**, 167–215.
43. Schwetlick, K. and W. D. Habicher (2002) Antioxidant action mechanisms of hindered amine stabilisers. *Polym. Degrad. Stab.* **78**, 35–40.
44. Brede, O. (1997) Time-resolved study of the antioxidant action of sterically hindered amines in alkane systems. *Radiat Phys Chem* **49**, 39–42.
45. Brede, O., D. Beckert, C. Windolph and H. A. Göttinger (1998) One-electron oxidation of sterically hindered amines to nitroxyl radicals: Intermediate amine radical cations, aminyl, α-aminoalkyl, and aminylperoxyl radicals. *J. Phys. Chem. A* **102**, 1457–1464.
46. Brede, O. and H. A. Göttinger (1998) Transformation of sterically hindered amines (HALS) to nitroxyl radicals: What are the actual stabilizers? *Angew. Makromol. Chem.* **261-262**, 45–54.
47. MacManus-Spencer, L. and K. McNeill (2005) Quantification of singlet oxygen production in the reaction of superoxide with hydrogen peroxide using a selective chemiluminescent probe. *J. Am. Chem. Soc.* **127**, 8954–8955.
48. Saito, K., K. Takeshita, J. Ueda and T. Ozawa (2003) Two reaction sites of a spin label, TEMPOL (4-hydroxy-2,2,6,6-tetramethylpiperidine-*N*-oxyl), with hydroxyl radical. *J. Pharm. Sci.* **92**, 275–280.
49. Nakamura, K., K. Ishiyama, H. Ikai, T. Kanno, K. Sasaki, Y. Niwano and M. Kohno (2011) Reevaluation of analytical methods for photogenerated singlet oxygen. *J. Clin. Biochem. Nutr.* **49**, 87–95.
50. Zalibera, M., P. Rapta, A. Staško, L. Brindzová and V. Brezová (2009) Thermal generation of stable $SO_4^{\bullet-}$ spin trap adducts with super-hyperfine structure in their EPR spectra: An alternative EPR spin trapping assay for radical scavenging capacity determination in dimethylsulphoxide. *Free Radic. Res.* **43**, 457–469.
51. Dodd, N. and A. Jha (2011) Photoexcitation of aqueous suspensions of titanium dioxide nanoparticles: An electron spin resonance spin trapping study of potentially oxidative reactions. *Photochem. Photobiol.* **87**, 632–640.
52. Bilski, P., K. Reszka, M. Bilska and C. Chignell (1996) Oxidation of the spin trap 5,5-dimethyl-1-pyrroline *N*-oxide by singlet oxygen in aqueous solution. *J. Am. Chem. Soc.* **118**, 1330–1338.
53. Diaz-Uribe, C., M. Daza, F. Martinez, E. Paez-Mozo, C. Guedes and E. Di Mauro (2010) Visible light superoxide radical anion generation by tetra(4-carboxyphenyl)porphyrin/TiO_2: EPR characterization. *J. Photochem. Photobiol. A: Chem.* **215**, 172–178.
54. Ijeri, V., K. Daasbjerg, P. Ogilby and L. Poulsen (2008) Spatial and temporal electrochemical control of singlet oxygen production and decay in photosensitized experiments. *Langmuir* **24**, 1070–1079.
55. Nizova, G., Y. Kozlov and G. Shuľpin (2004) Effect of acetonitrile on the catalytic decomposition of hydrogen peroxide by vanadium ions and conjugated oxidation of alkanes. *Russ. Chem. Bull.* **53**, 2330–2333.
56. Abellan, M., R. Dillert, J. Gimenez and D. Bahnemann (2009) Evaluation of two types of TiO_2-based catalysts by photodegradation of DMSO in aqueous suspension. *J. Photochem. Photobiol. A: Chem.* **202**, 164–171.
57. Mitroka, S., S. Zimmeck, D. Troya and J. Tanko (2010) How solvent modulates hydroxyl radical reactivity in hydrogen atom abstractions. *J. Am. Chem. Soc.* **132**, 2907–2913.
58. Cheng, Z., H. Zhou, J. Yin and L. Yu (2007) Electron spin resonance estimation of hydroxyl radical scavenging capacity for lipophilic antioxidants. *J. Agric. Food Chem.* **55**, 3325–3333.
59. Herscu-Kluska, R., A. Masarwa, M. Saphier, H. Cohen and D. Meyerstein (2008) Mechanism of the reaction of radicals with peroxides and dimethyl sulfoxide in aqueous solution. *Chem. Eur. J.* **14**, 5880–5889.
60. Dikalov, S. and R. Mason (2001) Spin trapping of polyunsaturated fatty acid-derived peroxyl radicals: Reassignment to alkoxyl radical adducts. *Free Radic. Biol. Med.* **30**, 187–197.
61. Dvoranová, D., V. Brezová, M. Mazúr and M. Malati (2002) Investigations of metal-doped titanium dioxide photocatalysts. *Appl. Catal. B: Environ.* **37**, 91–105.
62. Nosaka, Y., S. Komori, K. Yawata, T. Hirakawa and A. Nosaka (2003) Photocatalytic $^{\bullet}OH$ radical formation in TiO_2 aqueous suspension studied by several detection methods. *Phys. Chem. Chem. Phys.* **5**, 4731–4735.
63. Schwarz, P., N. Turro, S. Bossmann, A. Braun, A. Wahab and H. Durr (1997) A new method to determine the generation of hydroxyl radicals in illuminated TiO_2 suspensions. *J. Phys. Chem. B* **101**, 7127–7134.
64. Hirakawa, T., C. Koga, N. Negishi, K. Takeuchi and S. Matsuzawa (2009) An approach to elucidating photocatalytic reaction mechanisms by monitoring dissolved oxygen: Effect of H_2O_2 on photocatalysis. *Appl. Catal. B: Environ.* **87**, 46–55.
65. Lambert, C., H. Black and T. Truscott (1996) Reactivity of butylated hydroxytoluene. *Free Radic. Biol. Med.* **21**, 395–400.
66. Szabo-Bardos, E., K. Somogyi, N. Toro, G. Kiss and A. Horvath (2011) Photocatalytic decomposition of L-phenylalanine over TiO_2: Identification of intermediates and the mechanism of photodegradation. *Appl. Catal. B: Environ.* **101**, 471–478.